

Spin and charge dynamics in the Cu-O chains of $\text{YBa}_2\text{Cu}_4\text{O}_8$

F. Raffa, M. Mali, A. Suter, A. Yu. Zavidonov, J. Roos, and D. Brinkmann
Physik-Institut, Universität Zürich, CH-8057 Zürich, Switzerland

K. Conder

Laboratorium für Festkörperphysik, Eidgenössische Technische Hochschule Zürich, CH-8093 Zürich, Switzerland

(Received 8 February 1999)

We report an NQR-NMR study of the chain copper and apex oxygen in the high-temperature superconductor $\text{YBa}_2\text{Cu}_4\text{O}_8$. Above T_c , the temperature dependences of the Cu spin-lattice relaxation rate and the Knight shift are quantitatively described in the framework of the one-dimensional electron gas model, where the anisotropy and the correlation of the chain electron system are taken into account. Electric-field-gradient fluctuations due to charge carriers in the chains contribute partly to the chain Cu relaxation and dominate the apex oxygen relaxation. The different temperature dependences of the magnetic and quadrupolar relaxation rates of the chain Cu seem to confirm the separation of low-energy spin and charge excitations (spin-charge separation), expected in the framework of the one-dimensional electronic gas model. Finally, we present experimental evidence that below T_c the Cu-O chains become superconducting through the proximity effect.

[S0163-1829(99)03329-9]

I. INTRODUCTION

The high-temperature superconductor (HTSC) compounds $\text{YBa}_2\text{Cu}_3\text{O}_7$ (Y123 for short) and $\text{YBa}_2\text{Cu}_4\text{O}_8$ (Y124) contain single and double Cu-O chains, respectively. Even though these compounds are among the most widely studied of the HTSC, no established consensus has been reached for the ground state and the low-energy excitations of the single and double chains.¹⁻⁴

Because of the anisotropy of the electronic properties suggested by the crystalline structure and confirmed experimentally,^{5,6} the Cu-O chains present a good example of a quasi-one-dimensional (1D) electronic conductor. In the past two decades, 1D systems have been a playground for theoretical and experimental investigations of non-Fermi-liquid behavior. Indeed, strong electron-electron interactions present in 1D systems may lead to such a behavior and to the stabilization of a Luttinger-liquid state with the separation of low-energy charge and spin excitations.⁷

If probed by nuclear magnetic resonance (NMR) or nuclear quadrupole resonance (NQR), the chains of Y123 and Y124 do not exhibit simple metallic behavior. For instance, the Cu Knight shift varies linearly with temperature, and the spin-lattice relaxation rate, $1/T_1$, increases approximately with the temperature cubed, while, in a simple metal, the Knight shift is temperature independent and $1/T_1$ increases linearly with temperature.

In this paper, we describe an attempt to explain the puzzling behavior of the spin susceptibility of the chains in Y123 and Y124 by invoking the results of a theory treating nuclear spin-lattice relaxation in 1D conductors.⁸ This theory is based essentially on the results of the scaling theory for the quasi-1D correlated electron gas.⁹ It has been successfully applied to quasi-1D organic metals, like TMTSF and TMTTF salts,¹⁰ which are compounds made of weakly coupled organic metallic chains.

II. NMR-NQR BASIC CONCEPTS AND EXPERIMENTAL

We have performed temperature-dependent copper NQR and NMR and oxygen NMR experiments in Y124. For the chain Cu nuclei, we have determined the ^{63}Cu NQR frequency and linewidth (Figs. 1 and 2), and the ^{63}Cu and ^{65}Cu NQR spin-lattice relaxation rates, $1/T_1$ (Fig. 3), and the anisotropy of ^{63}Cu NMR $1/T_1$ (Table I). For the ^{17}O nuclei at the apex oxygen sites, we measured the NMR $1/T_1$ (Fig. 4) and, at 100 K, its anisotropy, and the magnetic shift (Fig. 5).

The ^{63}Cu NQR frequency is given by

$$\nu_Q = \frac{e^{63}QV_{zz}}{2h} \sqrt{1 + \frac{1}{3}\eta^2}, \quad (1)$$

where eQ is the ^{63}Cu quadrupole moment, V_{zz} is the largest principle component of the electric-field-gradient (EFG) tensor present at the Cu nucleus site, and η is the EFG's asymmetry parameter, which is nearly equal to one in our case.

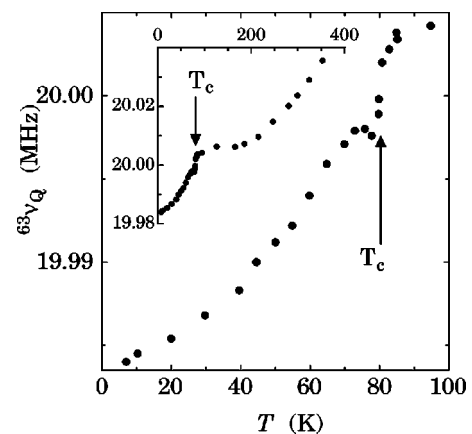


FIG. 1. Temperature dependence of the ^{63}Cu NQR frequency $^{63}\nu_Q$ below 100 K. The inset shows the whole data set.

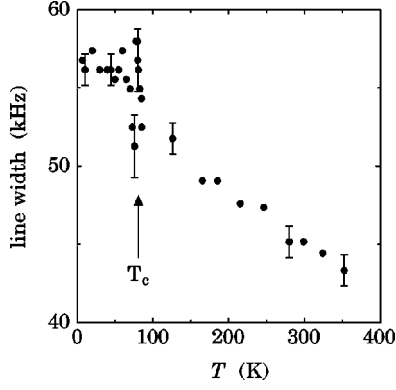


FIG. 2. Temperature dependence of the ^{63}Cu NQR linewidth defined as full width at half height.

The magnetic shift K^β of a NMR signal is measured when the external field is applied along the β direction. K^β is the sum of the temperature-independent orbital contribution K_{orb}^β and the temperature-dependent Knight shift $K_S^\beta(T)$, which is proportional to the static uniform electronic spin susceptibility (wave vector $q=0$, frequency $\omega=0$) χ_0^β :

$$K_S^\beta(T) = \frac{H_{\text{hf}}^\beta \mu_B^2}{2 \gamma_N \hbar} \chi_0^\beta, \quad (2)$$

where H_{hf}^β is the hyperfine field in the β direction.

The spin-lattice relaxation rate $1/T_1$ can be written as a sum of two contributions:

$$1/T_1 = R_M + R_Q. \quad (3)$$

The ‘‘magnetic relaxation rate’’ R_M is related to magnetic-field fluctuations at the nuclear site induced by the valence electron spins, while the ‘‘quadrupolar relaxation rate’’ R_Q is associated with EFG fluctuations which can arise from valence electron and/or ionic charges. In general, in NQR, the magnetic contribution R_M is given by the expression¹¹

$$R_M = 3k_B T (\gamma^2 / 2\mu_B^2) \sum_q F(q) \chi''(q, \omega_Q) / \omega_Q, \quad (4)$$

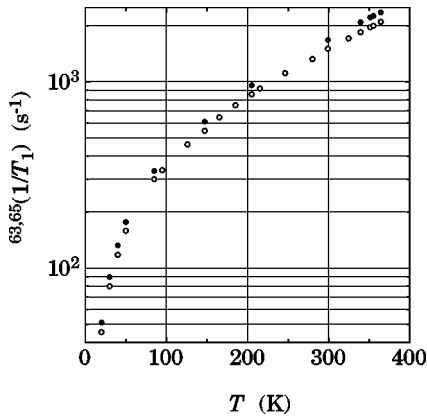


FIG. 3. Temperature dependence of the spin-lattice relaxation rate $1/T_1$ of ^{65}Cu (solid circles) and ^{63}Cu (open circles).

TABLE I. ^{63}Cu NMR spin-lattice relaxation rate data measured with the external field applied along the a , b , and c directions, respectively.

T (K)	$T_{1,a}$ (ms)	$T_{1,b}$ (ms)	$T_{1,c}$ (ms)
29	44.3	38.7	40.7
89	10.48	9.17	12.68
299	1.98	2.62	2.71

where $F(q)$, called the form factor, is the square of the Fourier-transformed hyperfine coupling constant, and $\chi''(q, \omega_Q)$ is the imaginary part of the dynamic spin susceptibility.

For details of the sample preparation and the performance of the experiment, we refer to Ref. 12. In the experiment reported in Ref. 12, the temperature had been monitored by means of the T -dependent ^{37}Cl NQR frequency of KClO_3 inserted in the Y124 sample. For technical reasons, in the present work we used the ^{35}Cl NQR line.

III. DATA ANALYSIS

A. Copper data above T_c

First, we decompose the Cu $1/T_1$ raw data (see Fig. 3) into the magnetic and quadrupolar contribution. This can be accomplished since R_M is proportional to the gyromagnetic ratio squared γ^2 , and R_Q is proportional to the quadrupole moment squared $(eQ)^2$. Writing Eq. (3) for both Cu isotopes, the following ratio can be formed:

$$\frac{^{65}T_1}{^{63}T_1} = \frac{^{63}R_M + ^{63}R_Q}{^{65}R_M + ^{65}R_Q} = \frac{1+y}{a+by}, \quad (5)$$

where the quotients $a = ^{65}R_M / ^{63}R_M = (^{65}\gamma / ^{63}\gamma)^2 = 1.1477$ and $b = ^{65}R_Q / ^{63}R_Q = (^{65}Q / ^{63}Q)^2 = 0.8562$ are known. Hence, $y = ^{63}R_Q / ^{63}R_M$ can be calculated. The results of the decomposition are shown in Fig. 6. Note that R_Q is about one order of magnitude smaller than R_M . The dashed line is a guide to the eye while the solid curve represents a fit to be discussed later.

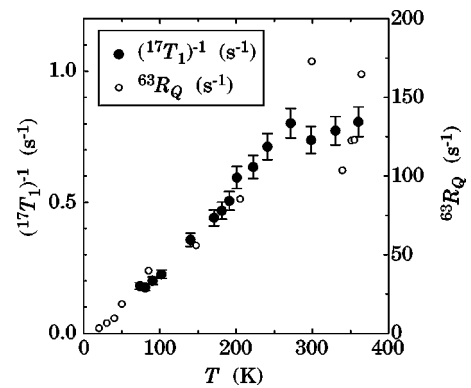


FIG. 4. Temperature dependence of the apical oxygen spin-lattice relaxation rate (solid circles) and the chain copper quadrupolar relaxation rate (open circles).

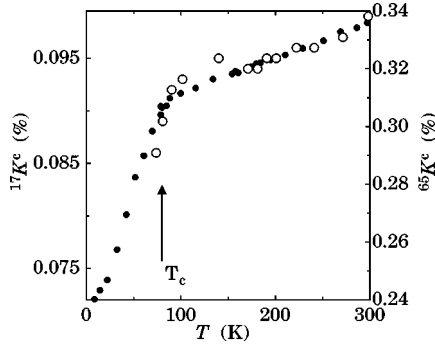


FIG. 5. Temperature dependence of the magnetic shift of the apical oxygen, $^{17}\text{K}^c$ (open circles), and of the chain Cu, $^{65}\text{K}^c$ (solid circles).

1. Magnetic relaxation

Most attempts made up to now to choose an appropriate microscopic model for describing the low-energy excitations of the Cu-O chains^{3,4,13} took into account the structural and electronic similarities between Cu chains and planes to take advantage of the huge number of theoretical and experimental studies of the Cu planes. Among others, the similarities of these two systems include the following facts: (i) In both systems, the Cu ion is coordinated by four oxygen ions; (ii) At half band filling, both systems behave as a spin- $\frac{1}{2}$ Heisenberg antiferromagnet;¹⁴ (iii) According to NMR results, each system has only one effective spin degree of freedom.¹⁵ Even though, in principle, a three-band model is a more realistic model, one-band models are simpler to study, and the one-band Hubbard model can reproduce the low-energy spectrum of the three-band model.^{16,17}

For these reasons, one-band models have been intensively used for the Cu-O planes and one may employ a single correlated band model also for the chains.

In view of the 1D character of the band and of the sizable electronic correlations, we consider the 1D electron-gas model⁹ as most appropriate to analyze our data. In this model, the direct electron-electron interaction is parametrized in terms of four coupling constants $g_{i=1,\dots,4}$ for left and right moving fermions. In the limit of the Hubbard model, these coupling constants all reduce to a single interaction parameter U . A peculiar characteristic of this model is

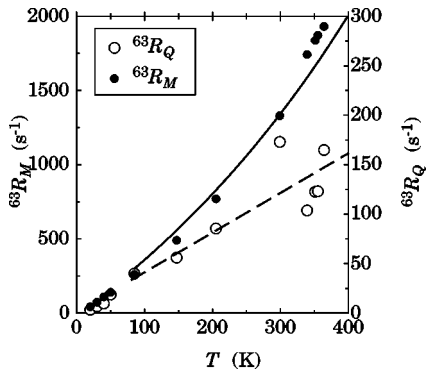


FIG. 6. Temperature dependence of the magnetic (R_M) and quadrupolar (R_Q) spin-lattice relaxation rate. The solid line is the result of the analysis described in Sec. III A 1. The dashed line is a guide to the eye.

the complete separation of long-wavelength charge and spin excitations, a phenomenon commonly called spin-charge separation.

We describe the chain 1D band energy dispersion by the expression typical for a 1D conductor

$$E(k) = 2t_{\text{eff}}[1 - \cos(kb_0)], \quad (6)$$

where b_0 is the lattice period and t_{eff} is an effective hopping integral. In the case of strong correlation, t_{eff} can be written as¹⁸

$$t_{\text{eff}} = \frac{2t}{1+c} \left\{ c + \left(\frac{1}{2} - \ln 2 \right) \left[(1-c)^2 - \frac{\sin^2 \pi c}{\pi^2} \right] \right\}, \quad (7)$$

where t is the hopping integral between nearest neighbors and c is the number of doped holes per chain copper-oxygen unit. Assuming that all copper ions in the chain are Cu^{2+} (Ref. 19) and the doped holes go into oxygen orbitals, one gets $c = 0.23$.²⁰

With $c = 0.23$, we obtain $t_{\text{eff}} = 0.2t$. In this case, one has $k_F = (\pi/2b_0)(1-c)$ and the Fermi energy E_F and the density of states per one spin direction $\rho(E_F)$ become

$$E_F = 2t_{\text{eff}}[1 - \cos[\pi(1-c)/2]] = 0.26t \quad (8)$$

and

$$\rho(E_F) = [2\pi t_{\text{eff}} \cos(\pi c/2)]^{-1} = 0.85/t, \quad (9)$$

respectively.

In a 1D metal, there are only two channels of magnetic relaxation: those induced by quasiparticles with $q \approx 0$ and $q \approx 2k_F$. We thus write

$$R_M = R_M(q \approx 0) + R_M(q \approx 2k_F), \quad (10)$$

where each term is given by Eq. (4) with the sums running over $q \approx 0$ and $q \approx 2k_F$, respectively.

The temperature behavior of the ($q \approx 0$) and ($q \approx 2k_F$) contributions have been determined by Bourbonnais who applied the scaling theory to the 1D electron-gas model.⁸ $R_M(q \approx 2k_F)/T$ decreases with increasing temperature, while $R_M(q \approx 0)/T$ increases and should dominate at sufficiently high temperature. In this model, $R_M(q \approx 0)$ is related to the uniform spin susceptibility, $\chi_0(T)$, by the following equations:

$$\chi_0(T) = 2\mu_B^2 \rho(E_F) / [1 - (2\pi v_F^*)^{-1} g_1(T)], \quad (11)$$

$$g_1(T) = g_1 / [1 + (\pi v_F^*)^{-1} g_1 \ln(E_0/2k_B T)], \quad (12)$$

$$R_M[q \approx 0] = \frac{3\pi H_{\text{hf}}^2 k_B T}{4\hbar \mu_B^2} \chi_0^2(T), \quad (13)$$

where $v_F^* = |dE/dk|_{k=k_F}$ is the electronic group velocity renormalized by umklapp processes and g_1 is the electron-electron coupling constant referring to backward scattering. E_0 is the bandwidth cutoff energy which determines the temperature dependence of the spin susceptibility. Bourbonnais assumed E_0 to be twice the *free*-electron Fermi energy, while we prefer to use E_0 as a free parameter. We stress that Eq.

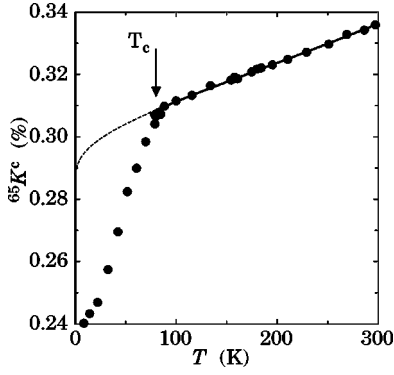


FIG. 7. Temperature dependence of the magnetic shift ${}^{65}K^c$ taken from Ref. 15. The solid line is the result of the analysis described in Sec. III A 1. The broken line is the extrapolation of the solid line for temperatures lower than T_c .

(13) is a consequence of the dimensionality and electronic correlation of the system, and it should not be confused with the Korringa relation.²¹

We will now show that the $R_M(q=0)$ contribution is dominating the magnetic relaxation in Y124 at high temperatures. In Fig. 7, we have plotted our earlier Cu Knight-shift data¹⁵ versus temperature. From T_c up to room temperature, which was the highest temperature reached in that experiment, K^c , and therefore $\chi_0(T)$, increases linearly with T . Most likely, the linear dependence extends up to 360 K, which is the highest temperature where we measured T_1 . In Fig. 8, the temperature dependence of both $(R_M/T)^{1/2}$ and $(1/T_1T)^{1/2}$ are displayed. Above 130 K, both quantities vary linearly with temperature. This is what one expects from Eq. (13) if the $q=0$ contribution prevails in the magnetic relaxation. By using previous relaxation data²² that extend up to 650 K, the inset of Fig. 8 shows that the linear relation of $(1/T_1T)^{1/2}$ with T holds even up to the highest temperature reached in those experiments.

The deviation of $(R_M/T)^{1/2}$, below 130 K, from a linear relation presumably comes from the increasing weight of the $2k_F$ contribution. The possibility that this deviation arises from a crossover to 3D correlations can be ruled out, since, in such a case, not only $(R_M/T)^{1/2}$ but also $\chi_0(T)$ and therefore K^c would change their temperature dependence.

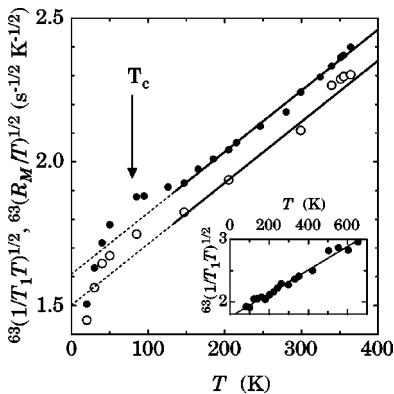


FIG. 8. Temperature dependence of ${}^{63}(1/T_1T)^{1/2}$ (solid circles) and ${}^{63}(R_M/T)^{1/2}$ (open circles) for chain copper. The solid lines are guides to the eye to stress the linear temperature dependence of the data above 130 K. The inset shows the corresponding Cu data of Ref. 22.

To check the consistency of the 1D electron-gas model, we extract quantitative information on the Cu chain system by fitting the Cu shift and relaxation data, ${}^{65}K^c$ and ${}^{63}R_M$, respectively, to Eqs. (2), (11), (12), and (13), where H_{hf} , c , g_1 , E_0 , t , and K_{orb}^c are adjustable parameters. However, for three of them we choose values known from other chain-plane experiments. We take $H_{\text{hf}}=A+2B\approx 120$ kOe/ μ_B by adopting the Y123 plane Cu values for both the on-site hyperfine field in the ab directions, $A\approx 31$ kOe/ μ_B , and the transferred field, $B\approx 43$ kOe/ μ_B .²³ For the on-site electronic repulsion, we take $U=5.4$ eV valid for the plane,¹⁷ and set $g_1=U=5.4$ eV (Hubbard model limit). As mentioned above, the value of c has been experimentally determined as $c=0.23$.²⁰ Thus, the fit of both the K^c and R_M data is performed with three adjustable parameters for which we obtained: $t=0.67$ eV, $K_{\text{orb}}^c=0.085\%$, and $E_0=0.34$ eV. The fit is remarkably good as seen in Figs. 7 and 6.

The numerical results of the fit agree very well with data obtained elsewhere. Our t value is very close to $t=0.82$ eV determined from the exact diagonalization for the Cu-O chain system in $\text{YBa}_2\text{Cu}_3\text{O}_{6+x}$.¹³ The E_0 value amounts to twice the Fermi energy of the *correlated* system, $E_F=0.17$ eV, obtained from Eq. (8), and not to twice the Fermi energy of the *free*-electron gas. Therefore, we suggest that the right choice for E_0 in Eq. (13) is $E_0=2E_F$.

2. Quadrupolar relaxation

There are various mechanisms which can be responsible for the relatively small quadrupolar contribution R_Q to the total Cu relaxation rate [see Eq. (3)]. If the relaxation were caused by phonons, one would expect the R_Q temperature dependence to obey a power law with a very large exponent at temperatures much below the Debye temperature, and a power *two* at temperatures above the Debye temperature.²⁴ Obviously, this is not what happens, rather the experimental data reveals a linear temperature dependence. Furthermore, the relaxation rate R_Q is too large to originate from phonons. Thus, we can safely exclude the phononic origin of the quadrupolar relaxation.

In a metal with non- s conduction electrons, the quadrupolar relaxation due to the charge carriers is finite and can be comparable to their magnetic dipolar contribution.²⁵ In the absence of other relaxation channels, we believe that this is the origin of the quadrupolar relaxation in the Cu chains. At this point we want to stress that R_M and R_Q have different temperature dependences as seen in Fig. 6. This different behavior, which is not expected for a simple metal, is an indication of the separation of spin and charge excitations expected in the framework of the 1D electron gas model. In such a case, R_Q would be related to the spectral density of holons. We will return to this point in Sec. III C.

B. Copper data below T_c

We now consider the chains at temperatures below T_c . The rapid decrease of the Knight shift, starting just at T_c (see Fig. 7), strongly indicates that at the superconducting transition, taking place in the Cu planes, also the chains get into a new state. The most natural explanation of this result would be that also the chains become superconducting, and this is due to the proximity effect. Since the superconducting state

is a 3D state, the chain electronic system, in order to become superconducting, has to switch from 1D to 3D behavior. This could happen through a 1D-3D crossover taking place above T_c , which, however, is unlikely, because K_S , and therefore χ_0 , retain their linear temperature dependence down to a few degrees above T_c . Hence, the most likely possibility is that, at T_c , the chains undergo a *transition* from a 1D to a 3D state, driven by the change in the electronic properties of the planes.

That the chain Knight shift drop at T_c relates to the superconducting transition in the planes, is also supported by the following facts. The presence of a sufficiently strong external magnetic field applied perpendicular to the chains along the a direction is able to suppress coherent transport along the c direction,⁵ i.e., to decouple the chains from the planes. Furthermore, the same external magnetic field suppresses the drop in the chain Knight shift, as it is clear from the chain Cu and O magnetic shift data in Ref. 15. These two facts together suggest that when the chains are decoupled from the planes by virtue of the external magnetic field, the new chain phase below T_c gets at least partially suppressed. This is consistent with the idea of superconductivity in the chains through the proximity effect.

Recently, Grévin *et al.*¹ have published convincing evidence for the presence of a charge-density wave (CDW) phase transition in the chains of $\text{PrBa}_2\text{Cu}_3\text{O}_7$. In a subsequent work,² they also suggest the presence of a CDW phase transition below T_c in the chains of Y1237, even though the evidence in this case is much less convincing. In case of Y124, the smooth passing of the chain Cu NQR linewidth across T_c (Fig. 2) does not lend support to the idea of a true CDW transition. In this case, below the CDW transition temperature, the CDW produced modulation of the EFG would distinctly show up in a sudden increase of the linewidth. This increase would be particularly evident since the chain Cu NQR linewidth of the present study is unprecedentedly narrow (Fig. 2). However, we cannot exclude the presence of short-range CDW correlations that slowly increase by decreasing temperature.

The small anomaly *and* the change in the temperature dependence of the NQR frequency detected at T_c (Fig. 1) must be connected with the lattice anomalies at T_c detected with various other experimental techniques.²⁶ They are the sign of a strong electron-phonon coupling of the electrons in the planes and, perhaps, in the chains. In Y123, a similar but larger anomaly at T_c in the chain Cu ν_Q has been found.²

There still remain some problems unresolved. For instance, the question why R_M is only slightly affected by the occurrence of superconductivity awaits an answer. In this context, it is interesting to note that, also below T_c , R_Q does not scale with R_M but seems to be suppressed more rapidly than R_M by the onset of superconductivity.

C. Apex oxygen data

The apical oxygen in high-temperature superconductors is probably the nuclear site least studied by NMR. The apex oxygen magnetic shift scales with the chain Cu magnetic shift (Fig. 5), but not with that of the plane. This indicates that the $2p$ apex oxygen orbitals overlap only slightly with the plane Cu $3d$ orbitals. Surprisingly, $1/T_1$ of apex oxygen

scales neither with chain Cu nor with plane Cu $1/T_1$, but with the quadrupolar relaxation R_Q of the chain copper (see Fig. 4). This implies that the electric-field-gradient fluctuations presumably induced by the holons in the chains (see Sec. III A 2) are also responsible for the apex oxygen relaxation.

That the apex oxygen relaxation is mainly of quadrupolar origin, is also supported by its anisotropy. At $T=92$ K, we measured the relaxation times $T_{1\alpha}$ with the external magnetic field applied in the α direction. For $\alpha=a,b,c$, we obtain the ratio

$$\frac{1}{T_{1c}} : \frac{1}{T_{1b}} : \frac{1}{T_{1a}} = 0.38 : 0.63 : 1,$$

where $T_{1c}=5$ s. At least three relaxation mechanisms are possible: first, the dipolar and, second, the transferred *magnetic* relaxation due to spin fluctuations of the quasilocalized copper $3d_{z^2-y^2}$ holes in the chains, and, third, the *quadrupolar* relaxation due to charge carriers. All these relaxation channels induce different anisotropies. While the transferred magnetic relaxation is expected to be almost isotropic, the other two are not. Let us assume an isotropically fluctuating magnetic moment at the Cu(1) site. It will produce, at the apex oxygen site, a fluctuating magnetic field whose c -axis component is twice as large as the others. For this reason, we expect for dipolar magnetic relaxation of the apex oxygen: $1/T_{1c} : 1/T_{1b} : 1/T_{1a} = 0.4 : 1 : 1$. For the quadrupolar relaxation anisotropy due to a breathing mode, we expect $1/T_{1c} : 1/T_{1b} : 1/T_{1a} = 0.02 : 0.7 : 1$ as described in the Appendix.

Both magnetic dipolar and quadrupolar mechanisms would induce a relaxation anisotropy not far from the one experimentally determined. We stress that in estimating the quadrupolar relaxation anisotropy, we used a crude approximation for the real fluctuations by considering only a *breathing* mode and assuming in-phase EFG fluctuations. In case of EFG fluctuations with symmetry lower than that of a breathing mode, $W_{2,c}$ would be increased with respect to the other two components, hence bringing the estimate closer to the experimental ratio. Thus, we conclude that only relaxation through quadrupolar interactions is able to explain consistently the temperature dependence *and* the anisotropy of the apex oxygen $1/T_1$.

This relaxation rate can be determined with quite a good accuracy, which contrasts with the difficulty of extracting reliably the quadrupolar contribution to the chain Cu relaxation, in particular at high temperature where the Cu magnetic relaxation background increases rapidly. Therefore, the information about the holon spectral density might be extracted with more precision from apex oxygen spin-lattice relaxation experiments to be performed in the future.

IV. CONCLUSION

We have shown that the static and dynamic spin susceptibility of the Cu chains in $\text{YBa}_2\text{Cu}_4\text{O}_8$ as determined by ^{63,65}Cu magnetic shift and spin-lattice relaxation rate can be described quantitatively within the framework of the 1D electron-gas model.^{9,8} In particular, the puzzling temperature dependence of the spin susceptibility is due to the low dimensionality and the electronic correlations of the system.

We have determined experimentally the temperature dependence of the Cu quadrupolar spin-lattice relaxation rate R_Q and ascribed it to the long-wavelength charge excitations of the system. The charge excitations, according to the 1D electron-gas model, are separated from the spin excitations (spin-charge separation).

The spin-lattice relaxation rate of the apical oxygen arises from the electric-field-gradient fluctuations caused by moving charge carriers in the chains. The chain Cu R_Q and the apex oxygen relaxation results wait to be compared with future theoretical predictions for the temperature dependence of the charge susceptibility in a 1D correlated electron gas.

Finally, we showed that the drop in the chain's magnetic shift at T_c seems to be related to the occurrence of superconductivity in the chains through the proximity effect. Our experimental findings are not compatible with a charge-density wave transition in the chains. Such a transition has been discovered in the chains of $\text{PrBa}_2\text{Cu}_3\text{O}_7$,¹ and has been suggested for the chains of $\text{YBa}_2\text{Cu}_3\text{O}_7$.²

ACKNOWLEDGMENTS

We acknowledge H. J. Schwer for carrying out x-ray-diffraction measurements, T. Ohno for collaborating in the setup of the NQR experiment, and A. Lombardi for performing preliminary measurements. The partial support of this work by the Swiss National Science Foundation, and in particular for K.C., is gratefully acknowledged.

APPENDIX: ANISOTROPY OF THE QUADRUPOLEAR RELAXATION IN THE CASE OF A BREATHING MODE

In this appendix, we will estimate the anisotropy of the apex oxygen relaxation if this arises from the ‘‘breathing mode’’ to be defined below. Within the framework of first-order perturbation theory, the transition probabilities W_1 and W_2 are related to the downward transition probabilities by²⁷

$$W_{m \rightarrow m-1} = W_1 \frac{(2m-1)^2(I-m+1)(I+m)}{2I(2I-1)^2},$$

$$W_{m \rightarrow m-2} = W_2 \frac{(I+m-1)(I-m+1)(I-m+2)(I+m)}{2I(2I-1)^2}.$$

W_1 and W_2 themselves are the Fourier transforms of the correlation function of the fluctuating EFG:

$$W_1 = \alpha \int_{-\infty}^{\infty} d\tau \langle V_{+1}(\tau) V_{-1}(0) \rangle \exp(-i\omega_{m-1,m}\tau),$$

$$W_2 = \alpha \int_{-\infty}^{\infty} d\tau \langle V_{+2}(\tau) V_{-2}(0) \rangle \exp(-i\omega_{m-2,m}\tau).$$

Here, $\langle \rangle$ signifies an ensemble average, $\alpha = (eQ/\hbar)^2$, and $\omega_{m-1,m}$ and $\omega_{m-2,m}$ are the frequencies for the corresponding transitions. $V_{\pm 1}$ and $V_{\pm 2}$ stand for the abbreviation

$$V_{\pm 1} = V_{xz} \pm iV_{yz},$$

$$V_{\pm 2} = \frac{1}{2}(V_{xx} - V_{yy}) \pm iV_{xy},$$

where the V_{ij} ($i, j = x, y, z$) are the components of the EFG tensor in a frame with the polar axis z parallel to the external magnetic field, B_0 .

In the following, we will assume that the EFG fluctuations do not affect the orientation of the EFG principle axis, that means the EFG tensor is not ‘‘tumbling’’ due to fluctuations. We will call such fluctuations the breathing mode.

For apex oxygen, the static principle axes of the EFG coincide with the crystallographic axes.²⁸ When applying B_0 along these axes, it follows immediately that $W_1 \equiv 0$ for a breathing mode because the V_{ij} , $i \neq j$ are exactly zero for this setup. Therefore, only W_2 remains to be estimated. Since the axes of the laboratory frame are a permutation of the principle axes of the EFG, the following relations hold:

$$W_{2,c} \propto (V_{x',x'} - V_{y',y'})^2, \quad B_0 \parallel c,$$

$$W_{2,a} \propto (V_{y',y'} - V_{z',z'})^2, \quad B_0 \parallel a,$$

$$W_{2,b} \propto (V_{z',z'} - V_{x',x'})^2, \quad B_0 \parallel b,$$

where primed variables refer to the frame of the principle axes of the EFG.

By using the static components of the EFG as determined by Mangelschots *et al.*,²⁸ we now can estimate the anisotropy of the quadrupolar spin-lattice relaxation of the apex oxygen. We get

$$W_{2,c} : W_{2,b} : W_{2,a} = 0.02 : 0.7 : 1.$$

¹B. Grévin, Y. Berthier, G. Collin, and P. Mendels, Phys. Rev. Lett. **80**, 2405 (1998).

²B. Grévin *et al.*, J. Supercond. (to be published).

³R. Fehrenbacher, Phys. Rev. B **49**, 12 230 (1994).

⁴S.-L. Drechsler, J. Málek, and H. Eschrig, Phys. Rev. B **55**, 606 (1997).

⁵N. E. Hussey, M. Kibune, H. Nakagawa, N. Miura, Y. Iye, and H. Takagi, Phys. Rev. Lett. **80**, 2909 (1998).

⁶I. Terasaki, N. Seiji, S. Adachi, and H. Yamauchi, Phys. Rev. B **54**, 11 993 (1996).

⁷J. Voit, Rep. Prog. Phys. **58**, 977 (1995).

⁸C. Bourbonnais, P. Wzietek, F. Creuzet, D. Jérôme, P. Batail, and

K. Bechgaard, Phys. Rev. Lett. **62**, 1532 (1989); C. Bourbonnais, J. Phys. I **3**, 143 (1993).

⁹J. Solyom, Adv. Phys. **28**, 201 (1979); V. J. Emery, in *Highly Conducting One-Dimensional Solids*, edited by J. T. Devreese, R. P. Evrard, and V. E. van Doren (Plenum, New York, 1979), Chap. 6.

¹⁰P. Wzietek, F. Creuzet, C. Bourbonnais, D. Jérôme, K. Bechgaard, and P. Batail, J. Phys. I **3**, 171 (1993).

¹¹T. Moriya, J. Phys. Soc. Jpn. **18**, 516 (1963).

¹²F. Raffa, T. Ohno, M. Mali, J. Roos, D. Brinkmann, K. Conder, and M. Eremin, Phys. Rev. Lett. **81**, 5912 (1998).

- ¹³A. A. Aligia, E. R. Gagliano, and P. Vairus, *Phys. Rev. B* **52**, 13 601 (1995).
- ¹⁴T. Ami, M. K. Crawford, and R. L. Harlow, *Phys. Rev. B* **51**, 5994 (1995); N. Motoyama, H. Eisaki, S. Uchida, *Phys. Rev. Lett.* **76**, 3212 (1996).
- ¹⁵M. Bankay, M. Mali, J. Roos, and D. Brinkmann, *Phys. Rev. B* **50**, 6416 (1994).
- ¹⁶E. Gagliano, S. Bacci, and E. Dagotto, *Phys. Rev. B* **44**, 285 (1991).
- ¹⁷M. S. Hybertsen, M. Schlüter, and N. E. Christensen, *Phys. Rev. B* **39**, 9028 (1989).
- ¹⁸H. Eskes, A. M. Oleś, M. B. J. Meinders, and W. Stephan, *Phys. Rev. B* **50**, 17 980 (1994).
- ¹⁹R. Fehrenbacher and T. M. Rice, *Phys. Rev. Lett.* **70**, 3471 (1993).
- ²⁰A. Krol, Z. H. Ming, and Y. H. Kao, *Phys. Rev. B* **45**, 2581 (1992).
- ²¹J. Koringa, *Physica (Amsterdam)* **16**, 601 (1950).
- ²²H. Zimmermann, M. Mali, D. Brinkmann, J. Karpinski, E. Kaldis, and S. Rusiecki, *Physica C* **159**, 681 (1989).
- ²³Y. Zha, V. Barzykin, and D. Pines, *Phys. Rev. B* **54**, 7561 (1996).
- ²⁴A. Abragam, *The Principles of Nuclear Magnetism* (Clarendon, Oxford, 1961); J. Van Kranendonk, *Physica (Amsterdam)* **20**, 781 (1954).
- ²⁵A. H. Mitchell, *J. Chem. Phys.* **26**, 1714 (1957); A. Narath and D. W. Alderman, *Phys. Rev.* **143**, 328 (1966).
- ²⁶For a summary of this effects, see, T. Egami and S. J. L. Billinge, in *Physical Properties of High Temperature Superconductors V*, edited by D. M. Ginsberg (World Scientific, Singapore, 1996).
- ²⁷K. Yosida and T. Moriya, *J. Phys. Soc. Jpn.* **11**, 33 (1956).
- ²⁸I. Mangelschots, M. Mali, J. Roos, D. Brinkmann, S. Rusiecki, J. Karpinski, and E. Kaldis, *Physica C* **194**, 277 (1992).